A tunable comb filter using single-mode/multimode/polarization-maintaining-fiber-based Sagnac fiber loop*

Ruan Juan(阮 隽), Zhang Wei-Gang(张伟刚)†, Zhang Hao(张 昊), Geng Peng-Cheng(耿鹏程), and Bai Zhi-Yong(白志勇)

Key Laboratory of Optical Information and Technology, Ministry of Education, Institute of Modern Optics, Nankai University, Tianjin 300071, *China*

(Received 17 September 2012; revised manuscript received 23 October 2012)

A novel tunable comb filter composed of a single-mode/multimode/polarization-maintaining-fiber-based Sagnac fiber loop is proposed and experimentally demonstrated. The filter tunability is achieved by rotating the polarization controller. The spectral shift is dependent on rotation direction and the position of the polarization controller. In addition, the adjustable range achieved by rotating the half-wave-plate polarization controller is twice higher than that of the quarter-wave-plate one.

Keywords: Sagnac fiber loop, filter, single-mode/multimode/polarization-maintaining-fiber, half-wave plate, quarter-wave plate

PACS: 42.79.Ci, 42.81.–I, 42.81.Gs **DOI:** 10.1088/1674-1056/22/6/064216

1. Introduction

Single-mode/multimode/single-mode (SMS) fiber structures have recently attracted considerable interest in the field of fiber-optic communications and sensing applications, owing to their simple structures and easy fabrication. A detailed theoretical study on the SMS structure regarding the refractive index distribution, influence of the type and concentration of dopants, and core diameter variation has been conducted.[1] These SMS structures have been extensively used in many fields.[1–5] Displacement sensing is obtained by using a bent SMS structure.[2] Hatta *et al.*,[3] measured the strain by using two SMS structures with a strain resolution of 0.34 $\mu\varepsilon$. The SMS combined with long period fiber grating (LPFG) and fiber Bragg grating (FBG) have been reported recently,[4,5] in which[4] a maximum coupling efficiency of 1.66% and a 3dB-bandwidth of 42 nm were achieved. More recently, SMS-structure-based coreless multimode fiber was reported with an ultra-high temperature sensitivity of 1880 pm/°C.[6]

The filter is an important component in the fields of optical communications, integrated optics, and wavelength division multiplexing (WDM).[7–9] A filter based on two-dimensional photonic crystal with elliptical-rod defects is proposed and the adjustability of the filter is obtained by changing the orientation angle of the elliptical-rod defects.[7] However, the dynamic adjustability cannot practically realized because it is rather difficult to experimentally control the orientation angle of the elliptical defects once the filter has already been fabricated. Jiang *et al.*[8] proposed a comb filter based on a twin-core fiber coupler and wavelength adjustability was achieved through CO_2 laser irradiation along the twin-core fiber. The extinction ratio is 25 dB and the wavelength spacing is 15 nm. However, the wavelength adjustability is nonreciprocal and costly due to the employment of an additional CO_2 laser system. Besides, a superstructure fiber Bragg grating comb filter was theoretically proposed and experimentally demonstrated.[9] However, it possesses a few disadvantages such as a complex fabrication system inability to dynamically adjust the transmission spectrum in real-time for commercial applications.

In this paper, we report on a tunable-wavelength comb filter based on multimode interference. The proposed filter comprises a single-mode/multimode/polarization-maintaining (SMP)-fiber-based Sagnac fiber loop, which has several advantages including easy fabrication, low-cost and real-time tunability. Its transmission spectrum shifts towards longer wavelength as the half-wave-plate polarization controller is rotated clockwise, whereas its transmission spectrum exhibits a blueshift for anticlockwise rotation. In addition, the spectral shift is dependent on the position of polarization controller and monotonically responds to the applied rotation angle.

2. Experiment and analysis

The experimental setup of the SMP-based Sagnac fiber loop is shown in Fig. 1(a) and the structure of SMP is shown in Fig. 1(c). The polarization controller (PC) comprises of two-quarter-wave plates (QWP) and a half-wave-plate (HWP) (see Fig. 1(b)). The wave plate is fabricated by coiling the fiber with selected N turns and a radius of R.[10] The phase delay between both modes of π or $\pi/2$ ($\lambda/2$ or $\lambda/4$ devices) could be obtained by reasonably selecting N and R.[10] The core diam-

*Project supported by the National Natural Science Foundation of China (Grant Nos. 11274181, 10974100, and 10674075), the Tianjin Key Program of Application Foundations and Future Technology Research Project, China (Grant No. 10JCZDJC24300), and the Specialized Research Fund for the Doctoral Program of Higher Education of China (Grant No. 20120031110033).

†Corresponding author. E-mail: zhangwg@nankai.edu.cn

© 2013 Chinese Physical Society and IOP Publishing Ltd

eter and the length of multimode fiber (MMF) used in our experiment are 50 μm and 13 cm, respectively. The polarization-maintaining-fiber (PMF) used in our experiment is a piece of PANDA PMF with a beat length of 3 mm at 1550 nm and a germanium-doped core and two boron-doped circular regions symmetrically located on both sides of the core. The length of PANDA PMF is 18 cm. When the light is injected from the input single mode fiber (SMF) into the MMF, multiple modes will be excited and will propagate within the MMF. As the light travels to PMF, some modes re-couple into core of PMF and others still propagate along the cladding of PMF. Two polarized light beams coming from the perpendicular direction interfere at 3-dB coupler output.

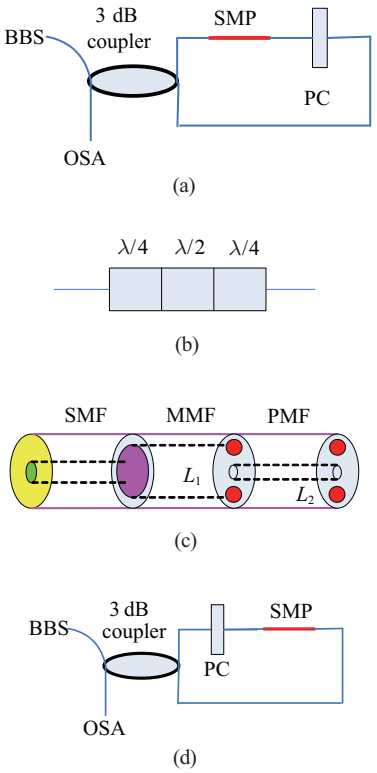


Fig. 1. (color online) Schematic diagrams of the proposed tunable filter (a), polarization controller (b), and SMP (c). BBS stands for broadband source and OSA the optical spectral analyzer.

The three wave plates (two quarter-wave-plates and a half-wave plate) are perpendicular to the horizontal plane and SMP is followed by PC. the spectrum of the proposed filter is shown in Fig. 2. Figure 2 shows that the fringe contrast and fringe spacing are 23.12 dBm and 14.1 nm at 1588.53 nm, respectively. In order to investigate the coupling between the core and cladding modes, the wavelength spectrum is converted into a frequency spectrum through fast Fourier transform. Figure 3 shows that a dominating cladding mode is excited by the multimode fiber. Then, we only clockwise rotate the HWP from the vertical position (90°) to the horizontal position (0°) and monitor the spectra with an OSA (AQ6370C) for different rotation angles. The experimental results show that the spectrum shifts towards longer wavelengths with clockwise rotation and that a spectral shift of 12.83 nm is obtained (see Fig. 4). The linear response of a spectrum shift to applied the rotation angle can be described by a fitting function of $y = 0.158x - 0.9421$ as shown in Fig. 5. Then, HWP is recovered to its original state (perpendicular to the horizontal plane). Similarly, we only anticlockwise rotate HWP from 90° to 180° and monitor the spectral shift. Figure 6 shows that the transmission spectrum shifts towards a shorter wavelength for anticlockwise rotation. Figure 7 shows that the linear response of a transmission spectrum to applied the rotation angle can be described by a fitting function of $y = -0.054x + 4.946$ in an angle rotation range from 100° to 150°.

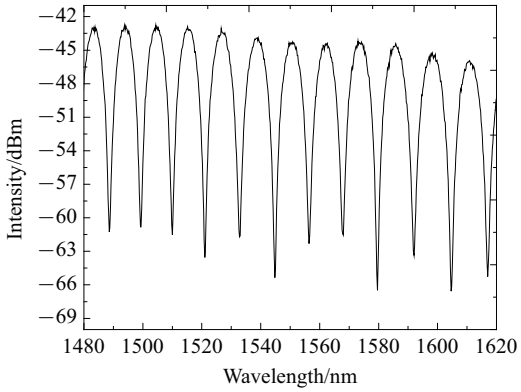


Fig. 2. Transmission spectrum of the Sagnac-fiber-loop-based filter.

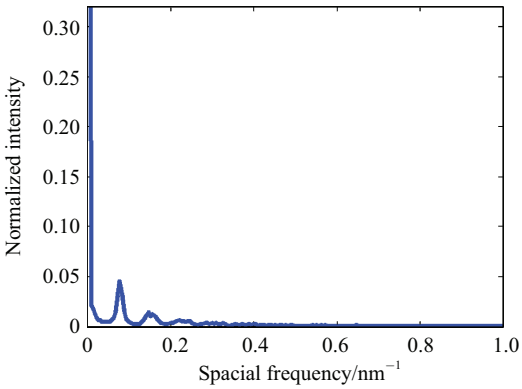


Fig. 3. (color online) Normalized intensity versus spacial frequency.

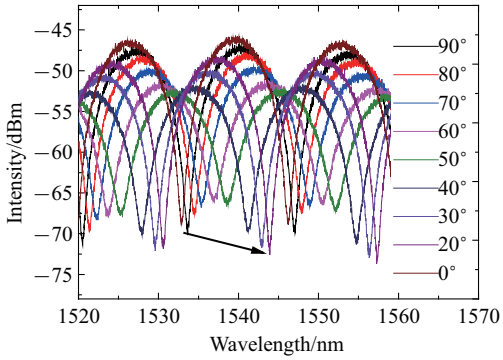


Fig. 4. (color online) Spectrum shifts for different clockwise rotation angles.

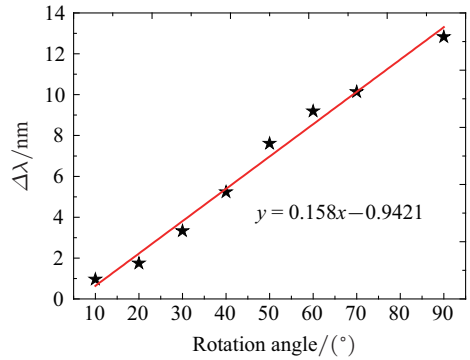


Fig. 5. (color online) Spectrum shift versus applied rotation angle.

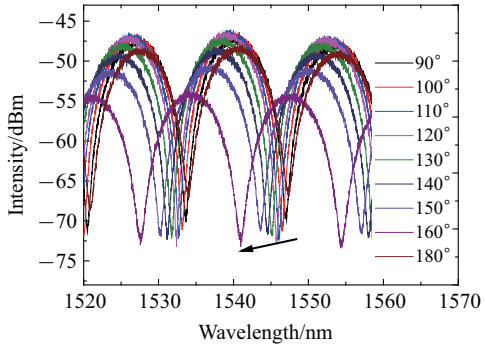


Fig. 6. (color online) Spectrum shifts for different anticlockwise rotation angles.

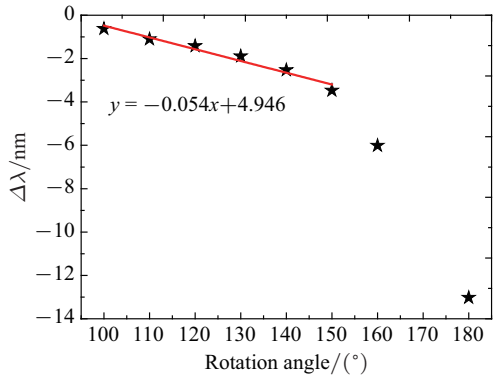


Fig. 7. (color online) Spectrum shift versus applied rotation angle.

After anticlockwise rotation measurements, HWP is recovered to its original state (perpendicular to the horizontal plane). Naturally, the influence of rotating QWP should be investigated. Therefore, we only clockwise rotate one QWP such as the left one in Fig. 1(b) from the vertical position (90°) to the horizontal position (0°). As shown in Fig. 8, the spectrum shifts towards a longer wavelength as the applied rotation angle changes and a redshift of 6 nm is experimentally obtained. After the QWP is recovered to its originate state, the same procedure is carried out for an anticlockwise rotation of the QWP. Figure 9 shows that the spectrum has a redshift as the anticlockwise rotation angle increases. Figure 10 shows that the transmission spectrum linearly shifts with an applied clockwise rotation angle and monotonically responds to an anticlockwise rotation angle. Here the clockwise rotation is positive and the anticlockwise rotation is set to be negative. The adjustable rotation range of the proposed filter using a HWP is twice higher than that using a QWP, which could be attributed to the fact that the phase delay of HWP is twice higher than that of QWP for the same rotation angle.

In order to investigate the dependence of transmission spectral characteristics on the spatial position of the combination of SMP and PC, we exchange the positions of the SMP and the PC. That is, the PC follows the SMP structure (see Fig. 1(d)). The same procedure mentioned above is conducted repeatedly. However, we find that the contrary experiment has opposite results. Figure 11(a) shows that the transmission spectrum shifts towards a shorter wavelength as HWP is only clockwise rotated.

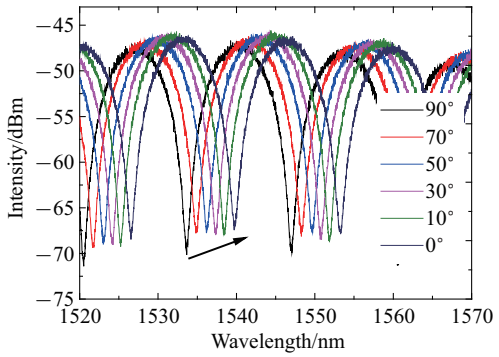


Fig. 8. (color online) Spectrum shifts for different clockwise QWP rotation angles.

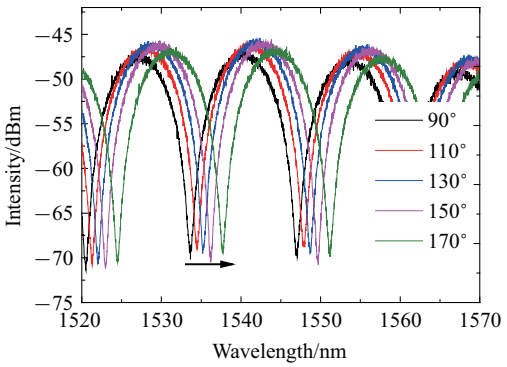


Fig. 9. (color online) Spectral shifts for different anticlockwise QWP rotation.

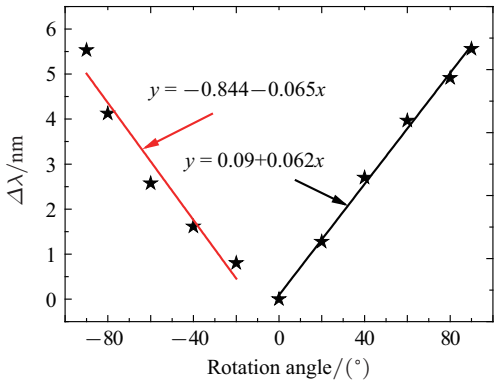


Fig. 10. (color online) Spectrum shift versus applied rotation angle.

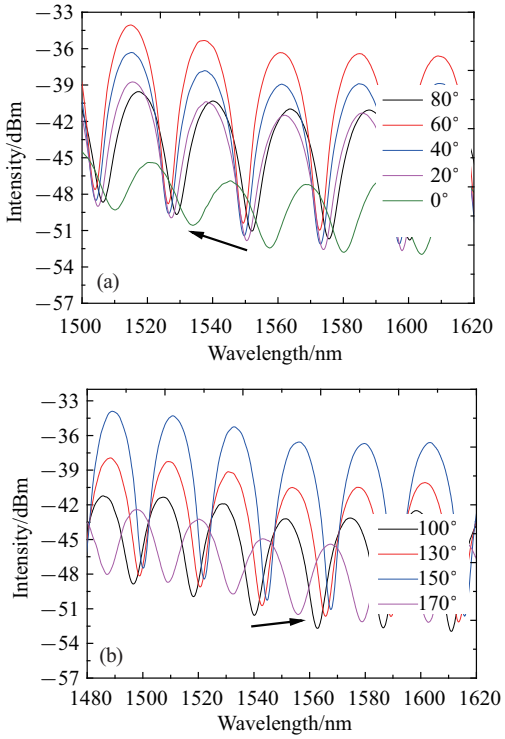


Fig. 11. (color online) Spectral shifts for different HWP rotation angles with the PC placed before the SMP. Panel (a) is for the clockwise rotation case, and panel (b) for the anticlockwise rotation case.

As shown in Fig. 11(b), the transmission spectrum exhibits a redshift as HWP is anticlockwise rotated. When the SMP is placed in front of the PC-based-Sagnac-fiber loop as shown in Fig. 1(a), we can only control the clockwise propagating polarization light by rotating the PC, which is caused by the PC-enabled polarization tunability of the clockwise propagating light inside the Sagnac fiber loop. Similarly, for the case of the PC placed in front of SMP (see Fig. 1(d)), we can only control the anticlockwise propagating polarization light by rotating the PC, which is caused by PC-enabled polarization tunability of the anticlockwise propagating light inside the Sagnac fiber loop. As is well known, inside a Sagnac fiber loop, the difference in phase between the clockwise propagating light and the anti-clockwise propagating light is π, and therefore, they exhibit an opposite spectrum shift response with the position of PC changing.

Since the core mode and a dominating cladding mode participate in the interference process, the transmission spectrum of the proposed filter can be expressed as[11]

$$I = I_1 + I_2 + 2\sqrt{I_1 I_2}\cos(\varphi), \tag{1}$$

where I_1 and I_2 represent the intensities of the core mode and a dominating cladding mode, respectively; φ is a phase difference induced by two polarized light beams propagating in PC and PMF and can be expressed as

$$\phi = \frac{2\pi}{\lambda}\left[N2\pi R(n_1 - n_2) + (n_\mathrm{f} - n_\mathrm{s})L\right], \tag{2}$$

where n_f and n_s are the refractive indices for the two perpendicular directions (fast axis direction and slow axis direction) of the PMF, respectively, L is the length of the PMF, N is the number of turns of fiber coils, and R is the radius of the fiber coils, n_1 and n_2 are the refractive indices of the fiber core and cladding, respectively.

The twist-induced elliptical birefringence changes the state of polarization (SOP) of the two polarization modes, resulting in the change of the coupling coefficient of the polarization mode. If the fiber is twisted, the SOP of the input light rotates with a rate of $\boldsymbol{\alpha} = g \cdot \boldsymbol{\tau}$ on the Poincaré sphere,[12] where g is the photoelastic coefficient and $\boldsymbol{\tau}$ is the twist rate vector (positive $\boldsymbol{\tau}$ denotes a clockwise twist and negative τ refers to an anti-clockwise twist). That is, the evolution of the SOP is proportional to the applied twist rate, and its rotation direction depends strongly on the twist direction. Therefore, the transmission spectral shift can be explained by the PC-rotation-induced evolution of SOP.

3. Conclusions

In the present paper, a tunable comb filter constituted by a single-mode/multimode/polarization-maintaining-fiber-based Sagnac fiber loop is proposed and experimentally demonstrated. Its transmission spectral shift is dependent on rotation direction and the position of the polarization controller. Furthermore, the tunable range achieved by rotating the half-wave plate is twice higher than that by rotating the quarter-wave plate. The proposed structure has several merits, including easy fabrication, low-cost, and real-time tunability, which makes it promising for potential applications in the field of fiber-optic communications and related areas.

References

[1] Tripathi S M, Kumar A, Varshney R K and Kumar Y B P 2009 *J. Lightwave Technol.* **27** 2348
[2] Wu Q, Semenova Y, Wang P, Hatta A M and Farrell G 2011 *Meas. Sci. Technol.* **22** 25203
[3] Hatta A M, Semenova Y, Wu Q and Farrell G 2010 *Appl. Opt.* **49** 536
[4] Wu Q, Semenova Y, Ma Y, Wang P, Guo T, Jin L and Farrell G 2011 *J. Lightwave Technol.* **29** 3683
[5] Wu Q, Semenova Y, Yan B, Ma Y, Wang P, Yu C and Farrell G 2011 *Opt. Lett.* **36** 2197
[6] Silva S, Pachon E G P, Franco M A R, Hayashi J G, Malcata F, Frazão O, Jorge P and Cristiano M B C 2012 *Appl. Opt.* **51** 3236
[7] Feng S and Wang Y Q 2011 *Chin. Phys. B* **20** 104207
[8] Jiang W W, Fan L Y, Zhao R F, Wei Y, Pei L and Jian S S 2011 *Acta Phys. Sin.* **60** 044214 (in Chinese)
[9] Cao H, Sun J Q, Zhang X L, Xiao L Y and Huang D X 2004 *Acta Phys. Sin.* **53** 3077 (in Chinese)
[10] Lefevre H C 1980 *Electron. Lett.* **16** 778
[11] Lim J L, Hu D J J, Shum P P and Wang Y X 2012 *IEEE Photon. J.* **4** 1163
[12] Ulrich R and Simon A 1979 *Appl. Opt.* **18** 2241